

Remagnetization in arrays of ferromagnetic nanostripes with periodic and quasiperiodic orderK. Szulc,¹ F. Lisiecki,² A. Makarov,^{3,4} M. Zelent,¹ P. Kuświk,^{2,5} H. Głowiński,² J. W. Kłos,^{1,6} M. Münzenberg,⁶ R. Gieniusz,⁷ J. Dubowik,² F. Stobiecki,² and M. Krawczyk¹¹*Faculty of Physics, Adam Mickiewicz University in Poznan, Umultowska 85, Poznań, 61-614, Poland*²*Institute of Molecular Physics, Polish Academy of Sciences, M. Smoluchowskiego 17, Poznań, 60-179, Poland*³*School of Natural Sciences, Far Eastern Federal University, Sukhanova 8, Vladivostok, 690091, Russia*⁴*Institute of Applied Mathematics, Far Eastern Branch, Russian Academy of Sciences, Radio 7, Vladivostok, 690041, Russia*⁵*Centre for Advanced Technologies, Adam Mickiewicz University in Poznan, Umultowska 89C, Poznań, 61-614, Poland*⁶*Institute of Physics, University of Greifswald, Felix-Hausdorff-Str. 6, Greifswald, 17489, Germany*⁷*Faculty of Physics, University of Białystok, Ciolkowskiego 1L, Białystok, 15-245, Poland*

(Received 8 October 2018; revised manuscript received 3 December 2018; published 12 February 2019)

We investigate experimentally and theoretically the magnetization reversal process in one-dimensional magnonic structures composed of permalloy nanostripes of the two different widths and finite length arranged in a periodic and quasiperiodic order. We showed that dipolar coupling between rectangular nanostripes is significantly reduced as compared to the analytical and numerical predictions, probably due to formation of the closure domains at the nanostripe ends. Although the main feature of the hysteresis loop is determined by different shape anisotropies of the component elements and the dipolar interactions between them, the quasiperiodic order influences the hysteresis loop by introducing additional tiny switching steps and change of the plateau width. We also showed that the dipolar interactions between nanostripes forming a ribbon can be counterintuitively decreased by reduction of the distance between the neighboring ribbons.

DOI: [10.1103/PhysRevB.99.064412](https://doi.org/10.1103/PhysRevB.99.064412)**I. INTRODUCTION**

Artificial spin systems (ASS), where large magnetic moments of the monodomain magnetic elements (MEs) significantly strengthen magnetostatic interactions with respect to the atomic systems, are interesting topic of research from fundamental physics and potential application points of view [1–4]. They allow to tailor influence of the long range interactions of the dipolar type on the ground magnetization state, where one of the interesting examples is frustration of the magnetization vector orientation appearing in the array of MEs arranged in the kagome or square lattice. There, the dipolar interactions between the monodomain MEs meeting at the vertex are modified due to proximity of the neighboring MEs and the reorientation of the magnetization near the edges [5,6]. The simple model of dipolarly coupled magnetic moments requires modification to take properly into account strength of the coupling [7]. Only recently, few ways of the magnetostatic coupling control between the MEs in the artificial spin ice systems have been demonstrated [8–10]. These discoveries give additional freedom for tailoring and tuning interactions of the magnetostatic origin and to study frustrated states.

The preferential axis of the magnetization orientation in the ME made of soft magnetic materials is determined by the shape anisotropy. Its magnetization reversal is affected also by the shape of the ME ends [11,12], roughness of the edges [13–15], and defects [16]. In the array of MEs, the magnetization reversal process is additionally influenced by the stray magnetic field from all other MEs in the array [17,18]. Interestingly, in the array the magnetostatic interactions from distant elements can result in indirect coupling

and even screening of the interactions from nearest elements. For this purpose, the inter-element spacing along the two perpendicular directions has been introduced in the triangular lattice of elongated MEs [19]. This large number of dependencies and competing interaction in the array makes the investigation of the remagnetization interesting. However, the results of experimental studies depend on the quality of the samples and defects inevitable in real samples. This makes the experimental results difficult to reproduce precisely in the numerical simulations [20].

Most of the investigations with ASS have been dealt with the periodic structures (PS), where every lattice point is equivalent [2]. The interesting question is, how the dipole interactions influence the magnetization reversal process in other, nonperiodic but ordered types of the ASSs, like the fractal or quasiperiodic structures (QPS). The expected hysteresis loop, due to variety of magnetization reversal processes, are difficult to predict [21–24]. Moreover, the quasiperiodic and fractal ASS are characterized by interesting spectra of the spin wave excitations, which can be controlled and modified by magnetization reversal process, which is potentially useful for applications in magnonics [25–31].

The ribbon of the magnetic nanostripes (NSs) is one of the simplest geometry. Nevertheless, it allows for systematic investigation of the complexity resulting from the long-range dipole interactions in periodic and nonperiodic structures [32–34]. In the paper, we investigate experimentally and theoretically the magnetization reversal process in the QPS consisting of the wide and narrow rectangular Py (Ni₈₀Fe₂₀) NSs of finite length collected into the ribbon, and also in the array of ribbons. We show that the interactions between

the NSs in the ribbon are significantly reduced close to the switching fields, as compared to the full saturated state. For comparable analysis of the magnetization reversal process in QPS, we fabricated the reference structures in the form of periodically ordered Py NSs. We show that despite of the reduced dipolar coupling between NSs in the experimental structures, the influence of the quasiperiodic order on the hysteresis loops is still visible. We also show that the separation between the ribbons, as well as an NS width, can be used to control the dipolar coupling between the NSs in the ribbon, and thus control the influence of the NS order on the magnetization reversal process.

The paper is organized as follows. In the next section, we describe the structures under investigations, and the theoretical models used to analyze the hysteresis loops measured experimentally. In Sec. III, we present the results of measurements, the analysis of the stray demagnetizing field during the remagnetization in PS and QPS, and Monte Carlo simulations result. In the last section, we summarize our study.

II. STRUCTURE AND METHODS

A. Structure

We fabricated the system of thin (thickness t) NSs from Py film on a silicon substrate using an electron-beam lithography and a lift-off technique. The narrow ($w = 350$ nm) and wide ($2w = 700$ nm) NSs of finite length L were arranged in the QPS according to the Fibonacci inflation rule [35]. The NSs are separated by $s_x = 100$ nm wide air gaps. The total quasiperiodic sequence of NSs ($100 \mu\text{m}$ long along the x direction) forms the ribbon. The ribbons are repeated periodically along the y axis into the array with air gaps s_y between them. The structure is drawn schematically in Fig. 1.

In order to investigate the influence of magnetostatic interactions between the NSs on a magnetization switching, we fabricated arrays with different structural parameters. In particular, we prepared the samples with NSs of thicknesses

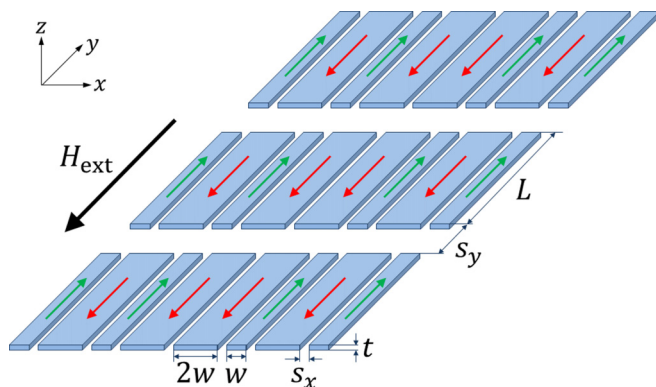


FIG. 1. Section of a considered quasiperiodic structure. The flat and long magnetic NSs of thickness t , widths w or $2w$, and length L ($t \ll w \ll L$) are placed side to side and separated by air gaps of the width s_x . The chains of NSs form the ribbons separated from each other by the gaps of the width s_y . The green and red arrows show the exemplary direction of magnetization in narrow and wide NSs, respectively. The external magnetic field (black arrow) is placed along the NS axis.

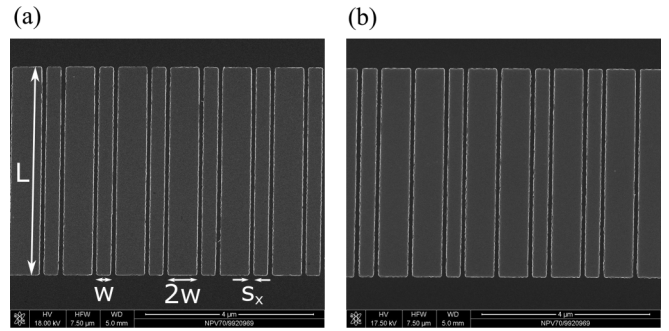


FIG. 2. The scanning electron microscopy images of a single ribbon formed by (a) periodic and (b) Fibonacci sequences of NSs.

$t = 30$ and 50 nm, lengths $L = 5 \mu\text{m}$ and $10 \mu\text{m}$, and with the separation between the ribbons $s_y = 760$ nm, $1.5 \mu\text{m}$, and $10 \mu\text{m}$. In our study, we kept the widths of NSs (w and $2w$) and the separation between them (s_x) unchanged. The whole size of the array of ribbons was about $100 \times 200 \mu\text{m}$.

We fabricated also the samples with a single ribbon and the samples with the arrays of ribbons formed by periodically ordered NSs. The PS was built by alternating repetition of the wide and narrow NSs. The fabricated structures can be seen in Figs. 2(a) and 2(b) where the selected scanning electron microscopy (SEM) images of the periodic and Fibonacci sequences of NSs are shown, respectively.

B. Experimental methods

We investigated the magnetization reversal process at room temperature using the microscopy based on longitudinal magneto-optical Kerr effect (L-MOKE). The measurements were done with the aid of a wide-field polarization microscope (modified Carl Zeiss Jenapol) equipped with a CCD camera. Hysteresis loops were obtained from the evolution of magnetic domain structure recorded while the external magnetic field H_{ext} was changing, being always applied along the NSs' easy axis (the y axis). We collected images of the selected ribbon placed in the middle of the array during few magnetization reversal processes to improve the signal-to-noise ratio. In an analysis of the magnetization switching of the individual NS in the ribbon, we took into account only wide NSs, because of the resolution of the microscope is not enough to reliably analyze the switching of the narrow NSs.

In a whole study, we observed only a full magnetization switching of the single NSs at given H_{ext} . At the fields H_{ext} close to the switching fields, we noticed small areas, near the ends of NSs, with a tilted magnetization direction (towards orientation parallel to the edge). However, this effect did not change the overall picture of abrupt magnetization switching in successive groups of the NSs with the change of H_{ext} .

C. Demagnetizing field of the single nanostripe

The basic element of the analytical model used in the paper is a rectangular stripe of width w , length L , and thickness t (Fig. 1). We assume that the NS is made of ferromagnetic material and it is homogeneously magnetized along

TABLE I. The switching field H_{sw} obtained from micromagnetic simulations (MS); the scaling factor κ of the magnetostatic interactions between NSs and anisotropy field H_{ani} derived from the linear regression (LR) analysis using Eq. (12) at four selected points of the hysteresis loop (see Fig. 3): I and II (III and IV) related to switching of the wide (the narrow) NSs.

| t (nm) | Parameter | Method | I | II | III | IV |
|----------|---------------------------|--------|-------|-------|-------|-------|
| 30 | κ H_{sw} (Oe) | LR | 0.034 | 0.046 | 0.114 | 0.116 |
| | | LR | 51 | 105 | 104 | 160 |
| | | MS | | 135 | | 295 |
| 50 | κ H_{sw} (Oe) | LR | 0.055 | 0.042 | 0.075 | 0.045 |
| | | LR | 42 | 82 | 123 | 182 |
| | | MS | | 135 | | 265 |

the y axis. Using the Maxwell equations in magnetostatic approximation:

$$\nabla \cdot (\mathbf{H}_{\text{demag}} + \mathbf{M}) = 0, \quad (1)$$

$$\nabla \times \mathbf{H}_{\text{demag}} = 0, \quad (2)$$

we can introduce magnetostatic potential $\mathbf{H}_{\text{demag}}(\mathbf{r}) = -\nabla\varphi(\mathbf{r})$ and derive the general formula for φ :

$$\varphi(\mathbf{r}) = -\int_V dV' \frac{\nabla' \cdot \mathbf{M}(\mathbf{r}')}{|\mathbf{r} - \mathbf{r}'|} + \oint_S d\sigma' \frac{\mathbf{n} \cdot \mathbf{M}(\mathbf{r}')}{|\mathbf{r} - \mathbf{r}'|}, \quad (3)$$

where V is volume of the NS, S is a surface of the NS, and \mathbf{n} is the vector normal to the NS surface pointing outside. Magnetic charges on the NS's sides perpendicular to the y axis can be considered as a source of the demagnetizing and stray fields, inside and outside of the NS, respectively. In Eq. (3), the part with the volume integral is equal to zero and only surface term contributes to the demagnetizing field. Eventually, formula for the field component parallel to the magnetization is described as follows [36,37]:

$$H_{\text{demag}}^i(\mathbf{r}, \mathbf{r}_i) = M_S \sum_{\alpha, \beta, \gamma=1}^2 (-1)^{\alpha+\beta+\gamma} \times \arctan \left[\frac{(x - x_i - x_\alpha)(z - z_i - z_\gamma)}{(y - y_i - y_\beta)|\mathbf{r} - (\mathbf{r}_i + \mathbf{r}'_{\alpha, \beta, \gamma})|} \right], \quad (4)$$

where $\mathbf{r}_i = (x_i, y_i, z_i)$ denotes position of the i th NS, $\mathbf{r} = (x, y, z)$, $\mathbf{r}'_{\alpha, \beta, \gamma} = (x_\alpha, y_\beta, z_\gamma)$, $x_1 = y_1 = z_1 = 0$, $x_2 = w$, $y_2 = L$, and $z_2 = t$. We neglect the components of the demagnetizing field perpendicular to the magnetization, because their average values are equal to zero inside the stripe. Equation (4) allows also to calculate the stray field produced by the i th NS, just by taking the location \mathbf{r} outside of the NS.

D. Monte Carlo simulations in the Ising model

To simulate the magnetization switching in magnetic NSs arranged in PS and QPS we examined the magnetic configurations and their energies using the Ising model. We considered the chain of dipolarly coupled macrospins in dependence on the strength of the external magnetic field. In our model, the wide and narrow NSs correspond to the macrospins of larger and smaller magnetic moments m_i , where i indicates the lattice site. The external field was applied perpendicular to the

chain, parallel to the macrospins. To take into account the difference in the shape anisotropy between the wide and narrow NSs, we lowered the external field at each macrospin by corresponding switching field of the NS. The switching fields $H_{sw,i}$ for a single (wide or narrow) NS were extracted from the hysteresis loops obtained from micromagnetic simulations (MSs) using MUMAX3 software [see Appendix and Fig. 8(a)] [38].

The computed values of the switching field collected in the Table I are significantly reduced in reference to the values of $H_{sw,i}$ predicted by the Stoner-Wohlfarth model [39], which assumes a monodomain and collinear magnetic configuration. This is because the magnetic configuration in areas close to the endings of NSs is noncollinear, with formation of closing domains [see the results of MS in Figs. 8(b)–8(g)]. This noncollinearity is restricted to a small volume of the NS, only slightly changes the value of the total magnetization. The magnetization reversal process of the single NS is very fast and happens in a single step of the external field.

This abrupt switching of the magnetization in a major part of the stripe [40] allows for treating the ferromagnetic NS as a macrospin in the following numerical simulations. In Ising model, we consider only two orientation of the macrospins: parallel (P) and antiparallel (AP) with respect to the external field, omitting the intermediate states, where the presence of barrier between those two states can be manifested directly (by taking into account anisotropy field). Therefore we decided to modify the Zeeman energy term by reducing the magnitude of the external field by switching field calculated numerically for single NS.

For every magnetic configuration in the considered Ising model, we compute the energy of dipolarly interacting magnetic moments in the external field:

$$E_l = \frac{1}{2} k \frac{\mu_0}{4\pi} \sum_{\substack{i, j \\ i \neq j}} \frac{m_i m_j}{|x_i - x_j|^3} - \sum_i m_i |H_{\text{ext}} - H_{sw,i}|, \quad (5)$$

where m_i takes the values $V_i M_S$ and $-V_i M_S$ for the P and AP alignments of the magnetic moment with respect to the external magnetic field direction, respectively. The symbol V_i is the volume of the i th magnetic NS and $M_S = 0.86 \times 10^6$ A/m is the saturation magnetization of Py. The symbol x_i denotes position of the i th magnetic moment.

In real samples, at the ends of NSs, a noncollinear magnetization configuration has been found in MS and magnetic force microscope images, which try to close the magnetic flux inside the magnetic structure and reduces the surface

charges. Therefore the stray magnetic field generated outside the magnetic NSs will be lowered [39], which can also significantly reduce the dipolar interactions between the NSs. In order to include this effect in simulations, we introduced in Eq. (5) the parameter k , which lowers the strength of dipolar coupling between magnetic moments in the simulating system ($0 \leq k \leq 1$).

We used the Monte Carlo (MC) method based on the METROPOLIS algorithm [41,42] to find the magnetic configurations which minimize the magnetic energy [Eq. (5)] when the external magnetic field is gradually changed. The details of the MC method with dipole interaction included can be found in Refs. [43,44] for different models. We used the Wang and Landau algorithm [45] where the relative probability of a transition from the configuration C_l of energy E_l to the configuration C_{l+1} characterized by energy E_{l+1} is given by the following formula:

$$P(C_l \rightarrow C_{l+1}) = \min \left[1, \exp \left(-\frac{E_{l+1} - E_l}{k_B T} \right) \right], \quad (6)$$

where T is a room temperature and k_B is Boltzmann constant. It means that in MC simulations the transition $C_l \rightarrow C_{l+1}$ is successful when the energy $E_{l+1} \leq E_l$, while for $E_{l+1} > E_l$, the transition happens with some probability exponentially decreasing with the energy difference. In order to draw the hysteresis loop, we changed the external magnetic field from 800 to -800 Oe and back, with 1 Oe step. At the limiting values of H_{ext} the system is magnetically saturated. In each step, i.e., for each considered value of the field, we find the magnetic configuration corresponding to the local energy minimum for all transitions from the configuration reached in the previous step. This quasiadiabatic change of the magnetic configurations induced by almost continuous variation of the H_{ext} allows us to determine the dependence of net magnetic moment on the external field: $M(H_{\text{ext}})/M_S = \sum_i m_i / \sum_i |m_i|$. Thus we are able to plot hysteresis loop and identify the metastable configuration, existing in specific ranges of an external field (examples of plotting a hysteresis loop using MC simulation are presented in the Refs. [46,47]). The numerical calculations were performed for PS and QPS composed of 144 magnetic moments, which is the number of NSs in the experimental structures.

III. RESULTS

A. Magnetization reversal process in L-MOKE measurements

In Fig. 3(a), we show comparison between the hysteresis loops for the arrays of ribbons of the Fibonacci QPS composed of NSs with $5 \mu\text{m}$ length, 50 nm thickness and for various separations between the ribbons $s_y = 760 \text{ nm}$, $1.5 \mu\text{m}$, and $10 \mu\text{m}$. For reference, we also place in Fig. 3(a) the outcomes for a single ribbon.

In all hysteresis loops, the two main steps of switching are clearly observed. The lower (higher) switching field is attributed to the magnetization switching in the wide (narrow) NSs, accordingly with their smaller (larger) shape anisotropy [48]. In arrays consisting of dipolarly coupled NSs, the magnetostatic interaction favors the AP magnetization orientation of the neighboring NSs [49]. For such configuration the lines

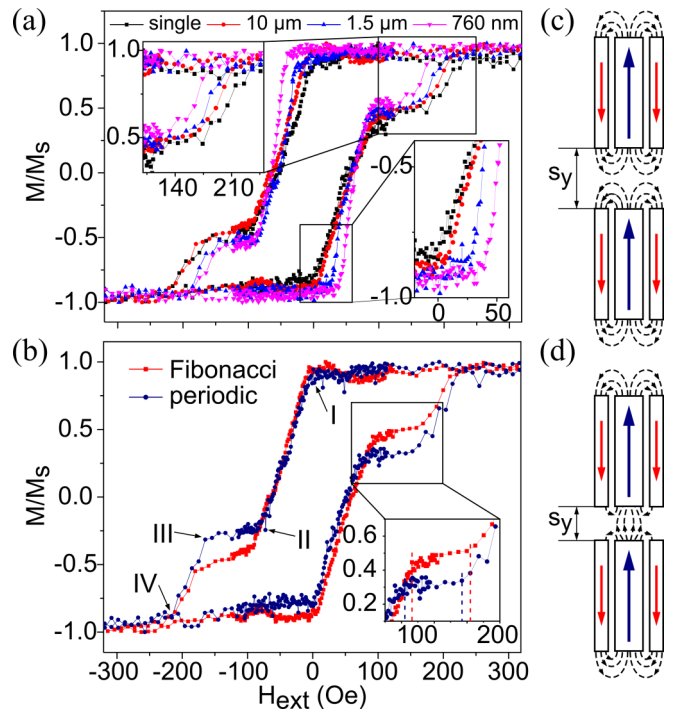


FIG. 3. Comparison of the hysteresis loops measured with L-MOKE in terms of (a) the separation between ribbons for the QPS with the NSs of $5 \mu\text{m}$ length and 50 nm thickness, and (b) for Fibonacci and PS array of NSs of $5 \mu\text{m}$ length, 50 nm thickness, and $10 \mu\text{m}$ separation between the ribbons. Vertical dashed lines in the inset mark the beginning and the end of the plateau. The labels I and II (III and IV) are related to switching of the wide (narrow) NSs. Scheme of the magnetic field lines from the wide NSs in the array when ribbons are well separated and close to each other are shown in (c) and (d), respectively.

of the stray magnetic field between the adjacent NSs are closed, which minimizes the magnetostatic energy of the system [50]. Thus the AP configuration stabilizes the system creating a plateau in the $M(H_{\text{ext}})$ dependence and the whole reversal process occurs in a wider magnetic field range. At higher switching field, we observe the transition from AP to P configuration related to the switching of narrower NSs.

By decreasing the distance between the ribbons, we can move the switching field of wide stripes to higher values [see the inset in the right-bottom corner in Fig. 3(a)], simultaneously the fields at which the narrow NSs switch are moving to lower fields [see the inset in the left-top corner in Fig. 3(a)], with differences reaching several dozens Oe.

When the ribbons are getting closer to each other the field lines from the NSs start to link the NSs from neighboring ribbons. As a result, the magnetic flux between the NSs in the same ribbon is lowered, as it is shown schematically in Figs. 3(c) and 3(d). This decreases the interactions between the NSs in the ribbon and reduces the width of the plateau related to the AP magnetization configuration. Interestingly, the distance $10 \mu\text{m}$ is usually considered to be sufficient for neglecting the magnetostatic interactions [51]. However, we still are able to observe some noticeable differences in the switching fields between a single ribbon and an array of ribbons with air gaps separating the ribbons up to $10 \mu\text{m}$.

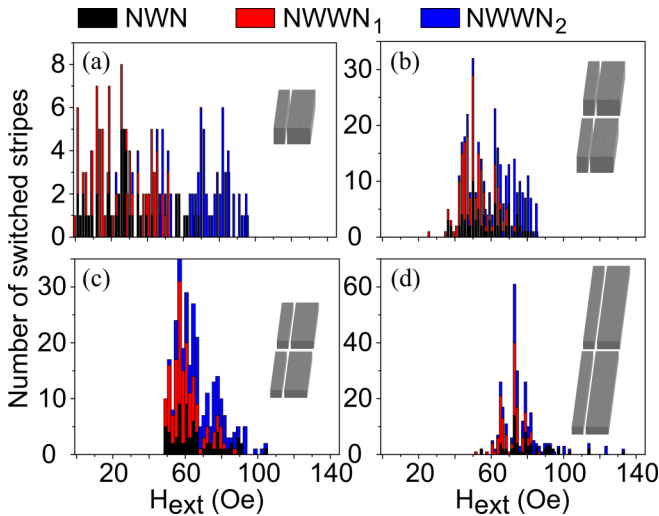


FIG. 4. Number of wide NSs (of 700 nm width), which are switched in successive intervals of external field for the Fibonacci QPS differing in the NS length / NS thickness / separation between ribbons: (a) $5 \mu\text{m}/50 \text{ nm}/\infty$ (single ribbon), (b) $5 \mu\text{m}/50 \text{ nm}/760 \text{ nm}$, (c) $5 \mu\text{m}/30 \text{ nm}/760 \text{ nm}$, and (d) $10 \mu\text{m}/30 \text{ nm}/760 \text{ nm}$. NWN is a wide NS between two narrow NSs, and NWWN₁ and NWWN₂ is a wide NS from a pair of two wide ones between the narrow NSs which is switched in a pair at a lower or higher field, respectively (see also the legend at the top of the figure for color bar definition).

Furthermore, we also find that for the sequences of thinner (or longer) NSs, we observe similar changes in the switching fields as described above, resulting from the decrease of the strength of the magnetostatic interactions between NSs inside the same ribbon [52].

In Fig. 3(b), we present comparison between hysteresis loops measured for the ribbons with $s_y = 10 \mu\text{m}$ separation composed of $5\text{-}\mu\text{m}$ -long and 50-nm -thick NSs with the periodic and quasiperiodic order. Slight differences between both curves are visible. The most significant difference is a magnetization value at the plateau. This is the effect of a different ratio of the wide to narrow NSs' numbers, which takes a value 1 for PS and $(1 + \sqrt{5})/2 \approx 1.618$ for QPS, and they correspond to plateau levels at the value 0.33 and $0.53M/M_S$, respectively. The other differences, which we will later relate to the different stray magnetic fields from the different arrangements, are seen at the beginning and at the end of the plateau phase [see, the inset in Fig. 3(b)].

For the quasiperiodic arrangement, we need a few Oe higher field to finish the switching of the magnetization in the wide NSs, than in a periodic structure. Also, the beginning of switching of the narrow NSs is at higher fields for QPS than for the PS.

Results presented in Fig. 4 show another interesting feature of the magnetization reversal process characteristic for the QPS. They are collected using the Kerr microscopy, and show how the wide NSs switch with the increase of external field. In QPS, the wide NSs appear in pairs surrounded by narrow NSs (marked as NWWN, which stands for the consecutive wires order: narrow, wide, wide, narrow) or be left as a single wide NS surrounded by narrow NSs on both sides (NWN: narrow,

wide, narrow). Generally, the magnetization of the first NS of the pair (NWWN₁) switches in a similar range of the external magnetic field to a single wide NSs (NWN). However, the second NS of the pair (NWWN₂) switches magnetization at a higher external magnetic field than the NWN. This indicates that there is a magnetostatic interaction between the pair of the wide NSs which introduces preferential AP configuration between wide NSs in the NWWNs. This effect is the most visible for the system with a single ribbon composed of $5\text{-}\mu\text{m}$ -long and 50-nm -thick NSs [Fig. 4(a)]. For this structure, the magnetostatic interactions between the NSs inside the ribbon is expected to be strongest among the systems presented in Fig. 4, thus the observed effect shall diminish for other structures, where interactions are decreasing.

Indeed, in Fig. 4 [and also in the inset at the right-bottom corner of Fig. 3(a)], it is clearly seen that the distribution of wide NSs switching fields narrows with decreasing the distance between the ribbons, i.e., when the magnetostatic interactions between NSs inside the ribbon decreases. In Fig. 4(a), the second NS from the pair (NWWN₂) reverses mainly in the range between 60 and 100 Oe, but this range becomes narrower and overlaps with the switching fields of the rest of the wide NSs with decreasing interactions between NSs, like in Fig. 4(b). With further lowering the interactions strength between the NSs, by decreasing thickness [Fig. 4(c)] or increasing length of the NSs [Fig. 4(d)], the switching range of wide NSs narrows and differences in switching fields between NWWN₁ and NWWN₂ vanishes. These effects do not occur in a PS, where there is no two wide NSs next to each other.

We showed that we can modify the strength of the magnetostatic interactions between the NSs in the ribbon in two ways: by changing the dimensions of the NSs (length or thickness) or by changing the distance between the ribbons. The decrease of the interactions between the NSs in the ribbon shall also decrease the differences between QPS and PS. These differences will be further investigated in the following parts of the paper with the use of the analysis of the stray magnetic field in the systems and MC simulations.

B. The structure field in the periodic and quasiperiodic sequence of nanostripes

We are going now to investigate quantitatively, based on the analytical approach presented in Sec. II C, the strength of dipolar interactions between selected NS and the other NSs in the structure at different points of the hysteresis loop (see Roman numerals in Fig. 3). This study shall give us additional information about the magnetization switching and the influence of geometrical parameters on this process [16,18].

We consider an array of rectangular prisms (Fig. 1), with dimensions and separating distances being the same as in the experimental samples. We take for calculations the ribbon made of 154 NSs for PS and 144 NSs for QPS. We use three different separations between the ribbons: 760 nm, $1.5 \mu\text{m}$, and $10 \mu\text{m}$, which are related to a different number of ribbons in the structure: 35, 31, and 13, respectively. There are two types of magnetization configurations that will be tested. First one, it is a P configuration, representing system at the beginning and at the end of magnetization reversal process, labeled

as I and IV, respectively. Second, is an AP configuration, corresponding to the plateau phase obtained in experimental results, at points labeled as II and III.

The total magnetostatic field H_{magn} can be expressed as a sum of the demagnetizing fields originating from individual NSs in the structure [calculated according with Eq. (4)]:

$$H_{\text{magn}} = \sum_j^{\text{all NSs}} H_{\text{demag}}^j. \quad (7)$$

The parameter, which we select for further analysis, is the stray magnetic field from all other NSs besides the considered i th NS, and it will be called the structure field:

$$H_{\text{str}}^i = H_{\text{magn}} - H_{\text{demag}}^i. \quad (8)$$

This field gives the information, how much of the magnetic field inside the selected NS is present due to interaction with other elements. We remind, the Eqs. (7) and (8) are derived under assumption of collinear magnetic configuration inside each NS.

First, we investigate H_{str} in the PS and QPS with different separations between the ribbons and for different configurations of the magnetization. We start from the P configuration, points I and IV, Fig. 5(a). There is no visible influence of the NSs order (periodic or quasiperiodic), which is in accordance the experimental results. Nevertheless, the increase of separation between the ribbons from 0.76 to 10 μm increases H_{str} by at least 500 Oe. Increase of H_{str} leads to decrease in H_{ext} at which switching happens. This explains the changes in the switching field at the beginning and at the end of the magnetization reversal process observed experimentally in Fig. 3(a).

The AP configuration is represented on hysteresis loops by the plateau phase, and so it starts at the end of magnetization reversal in the wide NSs [point II in Fig. 3(b)], and ends at the beginning of switching narrow NSs (point III). From the profile of the structure field calculated in the wide [Fig. 5(b)] and narrow NS [Fig. 5(c)] we see that the structure field in QPS is lower than in PS for both, wide and narrow NSs, which prefers remagnetization in QPS at higher H_{ext} . The differences in H_{str} between PS and QPS are especially visible in H_{str} of NWWN. The reason for this effect lies in the nearest neighbors of the wide NS in the QPS. In the QPS, the second stripe from the pair of wide NSs (NWWN₂) has lower H_{str} , than the single wide stripe (NWN).

C. Switching fields: theory and experiment

The total magnetic field inside selected NS is a sum of the external, magnetostatic and shape anisotropy field:

$$H_{\text{tot}} = H_{\text{ext}} + H_{\text{magn}} - H_{\text{ani}}. \quad (9)$$

We introduce the switching field in the way as it was computed in MS. It can be described as a function of internal magnetic fields:

$$H_{\text{sw}} = H_{\text{ani}} - H_{\text{demag}}. \quad (10)$$

Using Eqs. (10) and (8), we can rewrite Eq. (9) to the following form:

$$H_{\text{tot}} = H_{\text{ext}} + H_{\text{str}} - H_{\text{sw}}. \quad (11)$$

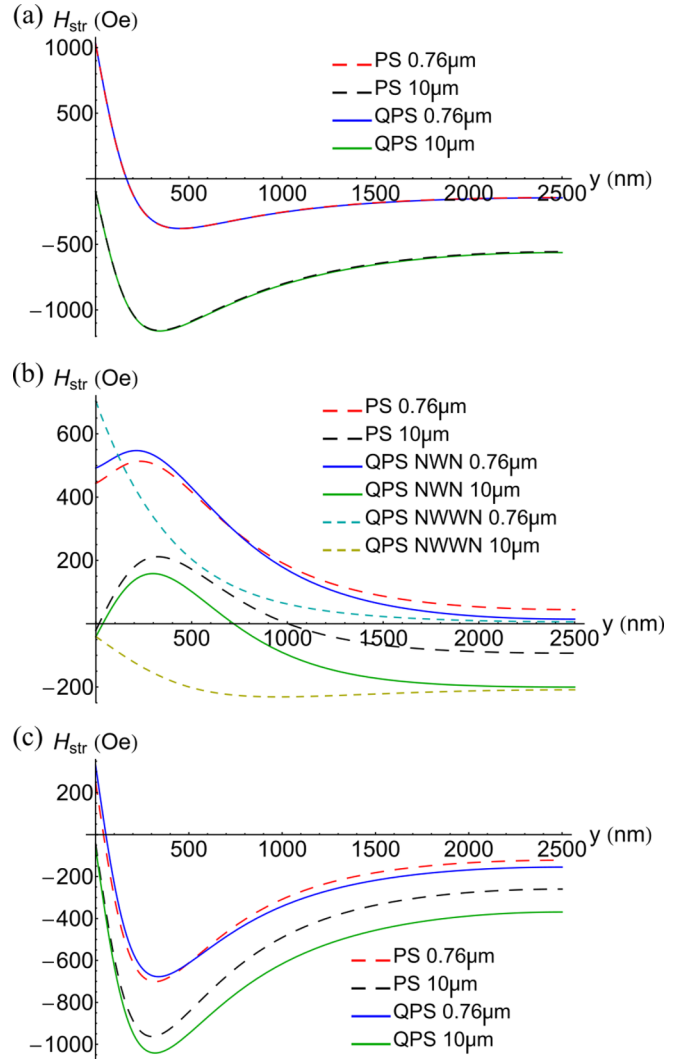


FIG. 5. The structure field H_{str} in the PS and QPS calculated for (a) a wide stripe (at NWN and NWWN positions) with P configuration of NSs, (b) a wide stripe (at NWN and NWWN positions) with AP configuration of NSs, and (c) a narrow stripe with AP configuration of NSs. The fields in (a), (b), and (c) are related to the points I, II, and III in the hysteresis loop marked in Fig. 3(a), respectively. The results for arrays of ribbons with the separation of 10 and 0.76 μm are marked with different colors. We plot H_{str} along the NS axis (along y axis) in the middle of the NS.

The experimental values of the external magnetic field H_{ext} at which selected NS switches and the structure field H_{str} obtained from the analytical model can be related to each other by the following equation:

$$H_{\text{ext}}(H_{\text{str}}^{\text{av}}) = -\kappa H_{\text{str}}^{\text{av}} + H_{\text{sw}}. \quad (12)$$

In Eq. (12), we used assumption that $H_{\text{tot}} = 0$ at the magnetization switching and $H_{\text{str}}^{\text{av}}$ is a structure field averaged over the volume of the NS under analysis. In Eq. (12), we have introduced the scaling factor κ to the structure field, similar to k in MC simulations in Eq. (5), to take into account the effect of magnetization curling at the ends of the NSs (found in measurements and visible in micromagnetic simulation

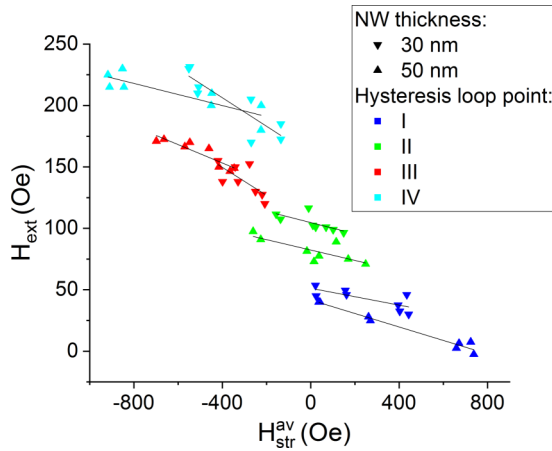


FIG. 6. Dependence of the external magnetic field at the selected points of the experimental hysteresis loop (I, II, III, and IV) where switching of the selected NS happens on the respective structure field calculated from the analytical model. The plotted lines are calculated regression lines from which the values of κ and H_{sw} were extracted and collected in the Table I. The results are shown for samples investigated experimentally in the paper.

results—Fig. 8) and different defects existing in the real sample, both leading to decrease of the stray field.

The collected values of H_{str}^{av} and related experimental H_{ext} fields at selected points of the hysteresis loop for PS, QPS, and various s_y form a functional dependence $H_{ext}(H_{str}^{av})$. Equation (12) can be treated as the equation of linear regression, and we can determine κ from a slope of the line approximating the function $H_{ext}(H_{str}^{av})$ and H_{sw} from intercept of the regression line with the H_{ext} axis. The obtained values of H_{sw} can be compared with the anisotropy field obtained from MS.

The experimental values of H_{ext} and the values of H_{str}^{av} at the magnetization switching at the characteristic points of the hysteresis loop (points I to IV), and for various structures, are collected in Fig. 6. The values of κ and H_{sw} obtained from linear regression analysis are collected in Table I. It confirms the presence of nonuniform magnetization in NSs, which strongly reduce dipolar interactions between them. Results show that κ does not depend strongly on dimensions of NSs (in Fig. 6, we distinguished two thicknesses 30 and 50 nm) and the separation between the ribbons. Nevertheless, κ has higher value in remagnetization of the narrow than of wide NSs, which points at large coupling at high magnetic fields. In most cases, κ is higher at the beginning than at the end of the magnetization reversal process in the NSs of given width. We can point out that stronger interactions between NSs yield faster remagnetization process.

The values of H_{sw} from regression analysis are much lower in comparison to magnetic anisotropy obtained from MS. We can attribute it to the edge roughness and remagnetization process through magnetization rotation starting at the NS edges, which can influence effective anisotropy and consequently decrease H_{sw} [13,20]. In each case, H_{sw} obtained from the regression is higher at the end than at the beginning of the magnetization reversal process in NSs of a given width, when it should be constant for all NSs of the same geometry in the ideal structure. This result leads to the conclusion that the

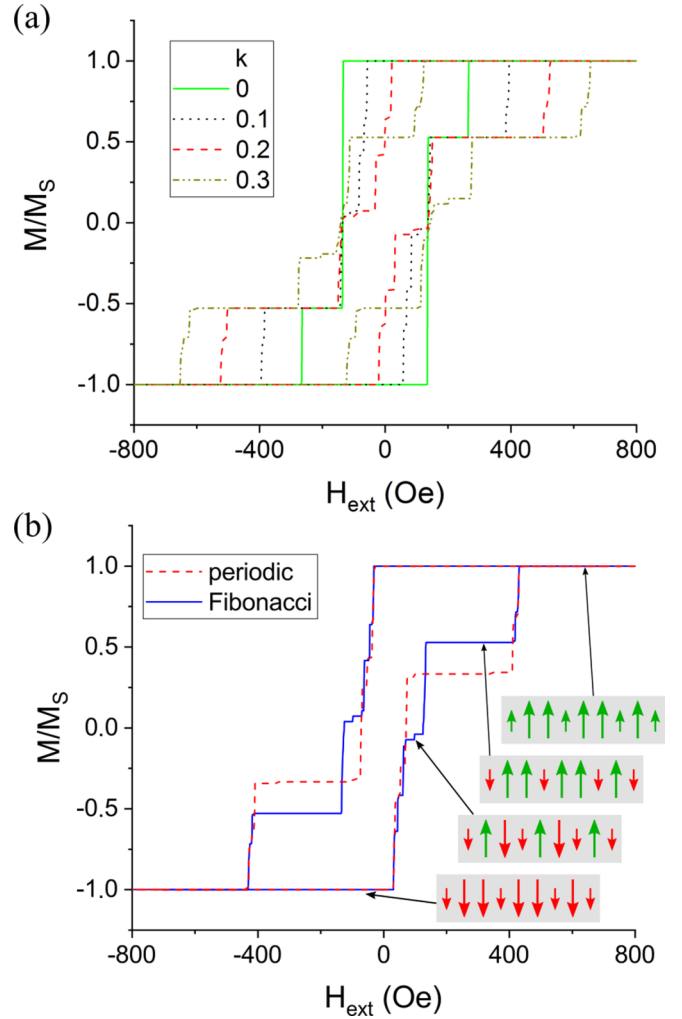


FIG. 7. Comparison of the hysteresis loops obtained from MC simulations. For (a) the single Fibonacci chain of magnetic moments corresponding to $5\text{-}\mu\text{m}$ -long and 50-nm -thick NSs for different values of the k parameter and (b) for the periodic and Fibonacci sequence of the magnetic moments, corresponding to $5\text{-}\mu\text{m}$ -long and 50-nm -thick NSs at k fixed to 0.1.

experimental switching field can differ between NSs, which could be the effect of different level of defects in NSs [14,15].

D. Monte Carlo simulations of the remagnetization

In Fig. 7(a), we present the influence of dipolar interactions strength on the hysteresis loop obtained in MC simulations. For noninteracting NSs ($k = 0$) the remagnetization follows the two steps process, separated by the plateau of the width equal to the difference between the switching fields of the isolated wide and narrow NS. An increase of the parameter k makes the plateau wider. Magnetization reversal process of the narrow stripes moves to higher values of H_{ext} with increasing k , while for the wide NSs the field of the switching beginning moves to lower values. Interestingly, the beginning of the plateau (the end of the wide NSs switching) remains almost on the same position. Nevertheless, the plateau is enlarged with increasing interactions between magnetic moments. According to the MC simulations, the magnetization of

the narrow NSs in PS and QPS switches at significantly higher values in reference to the values reported in the experiment [Fig. 3(b)]. We associate this difference with too high magnetic switching fields assumed for single NS, which can be related to the regular rectangular shape used in MS, a lack of defects and probably overestimated magnetization saturation in simulations.

In Fig. 7(a), we can see additional narrow plateau for QPS at the level of $M = 0.05M_S$ for $k = 0.1$ and 0.2 , which enlargers with k , and represents magnetization state, where only the second from the pair of the wide NSs (NWWN₂) has not yet been switched. In Fig. 4, we have seen that the behavior of the experimental system is similar. Lack of a clear plateau in the experiment can be associated with defects and deviation from the rectangular shape of the NSs, which facilitate nucleation of the reversal process and influence the switching process. Detailed inspection of Fig. 7(a) for $k = 0.1$ and 0.2 allows to identify also some additional steps in the reversal of the wide NSs (at $M = 0.4M_S$ and $0.6M_S$) and narrow NSs (at $M = 0.65M_S$). They point at the parts of the hysteresis loop where an influence of the long-range order can be expected, whenever the effective magnetostatic interactions between NSs will be sufficiently strong. Interestingly, for very strong dipolar interactions $k > 0.25$, the scenario of the remagnetization changes, see the curve for $k = 0.3$ in Fig. 7(a). In this case, the stray field from wide NSs prevail the shape anisotropy of the narrow NSs, and the magnetization reversal process tends start from the switching of the narrow NSs already before H_{ext} reaches 0. However, such strong dipolar interactions are not accessible in our experiments.

To make rough comparison of the MC results with experimental data, we have to select the k value for which the agreement would be reasonable. It can be done in two ways. Using difference between centers of remagnetizations of wide and narrow NSs, or using widths of remagnetization processes of wide and narrow NSs. The first approach gives us the value of $k \approx 0.03$, the second results in $k \approx 0.05$ and ≈ 0.1 for wide and narrow NSs, respectively. Those k values are of the same order as κ parameter collected in Table I estimated from the regression analysis in Sec. III C.

The few factors contribute to the low value of k in our system. One is associated with the stray field produced at the ends of the stripes. Even for a magnetic configuration where the net magnetization along the easy axis is reduced only slightly, the stray magnetic field outside of the stripe can be significantly lowered. Such a situation happens when the magnetization is tilted at the terminations of the stripe, in a small volume [see Figs. 8(b)–8(g)]. We made the additional MSs of magnetization reversal of the single NS. For the external magnetic field, just before magnetization switching, the stray field is reduced by about a quarter of the value as compared to the full saturation state at high field, while the total magnetization is reduced less than 10% for the wide NS (and an even smaller amount in the narrow NS). The tilting of the magnetization at the NS ends can be influenced by many factors besides the demagnetizing field of rectangular ends assumed in simulations, like the shape of ends [11, 12], rounded corners, roughness [13, 15], modification in the patterning process of the material at the NS edges. Another additional reason of low value of k is probable overestimation of the saturation

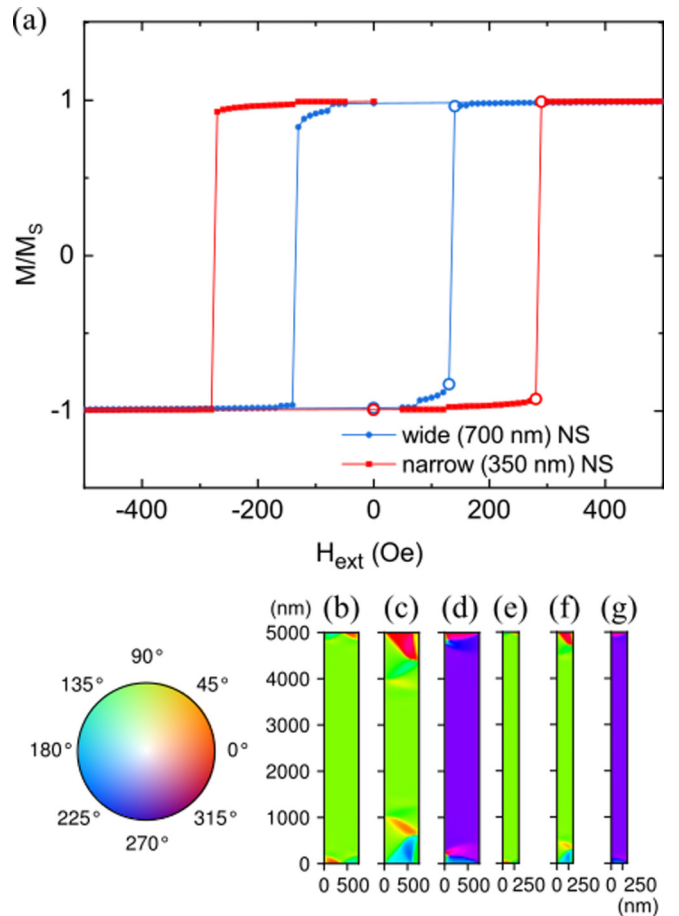


FIG. 8. Results of the micromagnetic simulations. (a) Hysteresis loops for the single wide (700 nm) and narrow (350 nm) NS. The empty circles point at the fields for which the magnetization configuration is shown in (b)–(g). [(b)–(d)] Magnetization inside of the wide NS at (b) 0, (c) 130, and (d) 140 Oe. [(e)–(g)] The magnetization configuration inside a narrow NS at magnetic fields (e) 0, (f) 290, and (g) 300 Oe. The color indicates the orientation of the magnetization in the NS plane according with the color map shown in the inset. The intensity show the magnetization orientation in the plane perpendicular to the plane of NS, with the white color marked orientation perpendicular to the plane of the NS.

magnetization M_S of Py. For calculations and simulations, we took the bulk value $M_S = 0.86 \times 10^{-6} \text{ A m}^{-1}$. However, in thin patterned films, it can be noticeably reduced. We estimate that it can give an additional 10%–20% reduction of parameter k . Finally, it is worth noting that only at the external fields close to the coercive fields of isolated NSs, the parameter k can influence the magnetization switching and exactly in this range of the external field we found lowered k and κ values.

In Sec. III A, we discussed that decrease of the separation between ribbons results in weakening of interactions between NSs in the ribbon [see Figs. 3(c) and 3(d)]. The same effects should be observed with lowering the value of k in MC simulations, and indeed, MC simulations confirm this hypothesis. Finally, we have made comparison of the hysteresis loops for the PS and QPS obtained from MC simulations. We select $k = 0.1$, which is close to the interactions strength in the experimental structure. The results are shown in Fig. 7(b).

According with expectations, there is no additional plateau phase in the PS, which is associated with lack of the pairs of wide NSs. Thus the wide NSs end their remagnetization at higher H_{ext} in QPS than in the PS, just as it was found in the experimental results shown in Fig. 3(b).

IV. CONCLUSIONS

We have investigated experimentally the hysteresis loops and magnetization switching for the arrays of Py NSs in dependence on the strength of magnetostatic interactions between the NSs and the type of the NS arrangement. We have studied ribbons with periodic and quasiperiodic sequences of wide and narrow NSs. We have modeled the dipolar interactions in the considering systems in a fabrication process. We have used the arrays differing in length, thickness of the NSs, and the distance between the adjacent ribbons. For explanation of the experimental results, we have conducted the numerical studies based on the Monte Carlo simulations for the macrospin Ising model. The numerical computations and experimental studies have been supplemented by detailed analytical investigations of the dipolar fields at different points of the hysteresis loop.

We have shown that the dipolar interactions in the experimental system of coupled NSs are strongly weakened as compared to the macrospin model. We attribute this decrease to the formation of the closure domain at the NS ends and thus significant decrease of the stray magnetic field from NSs. We have shown that the remagnetization process can be controlled by various geometrical parameters with the most relevant changes obtained by varying the separation between the ribbons. With decreasing this separation, the magnetostatic coupling between the NSs in the ribbon is significantly reduced. Moreover, the results show that the influence of the neighboring ribbons on the remagnetization can be detectable even at separation as large as $10 \mu\text{m}$. The change of the NS thickness and length offer the other possibilities to influence the magnetostatic interactions between the NSs.

We have found differences between remagnetization processes in the periodic and Fibonacci sequences of NSs. The main difference results from the presence of the pairs of wide NSs in the quasiperiodic structure, where due to the preferential antiparallel orientation of the magnetization in those pairs, the additional step in the hysteresis loop can exist. There are also more subtle effects demonstrated in Monte Carlo simulations, however they are hindered in experiment due to weakened magnetostatic coupling. Reduction of defects and optimization of the shape can enhance dipolar coupling between the NSs in the ribbon and enable experimental observation of the features in hysteresis loops characteristic for QPS.

ACKNOWLEDGMENTS

The research has received funding from the European Union's Horizon 2020 research and innovation pro-

gramme under the Marie Skłodowska-Curie Grant Agreement No. 644348, and W28/H2020/2017 from the Polish Ministry of Science and Higher Education resources for science in 2017-2019, and by the National Science Centre Poland for Grants No. 2015/17/B/ST3/00118, No. 2016/21/B/ST3/00452. J.W.K. would like to acknowledge the financial support of the Foundation of Alfred Krupp Kolleg Greifswald. A.M. thanks the Russian Foundation for Basic Research (research Project No. 18-32-00713) and the Michail-Lomonosov-Programme for the German-Russia promotion of science and the German Academic Exchange Service (DAAD). The simulations were partially performed at the Poznan Supercomputing and Networking Center (Grant No. 209).

APPENDIX: MICROMAGNETIC SIMULATIONS OF A SINGLE NANOSTRIPE

Micromagnetic simulations were performed for a finite $350 \times 5000 \times 30 \text{ nm}$ and $700 \times 5000 \times 30 \text{ nm}$ rectangular stripes using a uniformly discretized grid with the size of the cell $1 \times 5 \times 10 \text{ nm}$. We used the standard Py magnetic parameters for magnetization saturation $M_S = 0.86 \times 10^6 \text{ A/m}$, exchange stiffness constant of $A = 1.3 \times 10^{-11} \text{ J/m}$, and Gilbert damping parameter $\alpha = 0.01$. The initial magnetization was set to a random magnetization. Hysteresis loops were simulated for the external magnetic field directed along the NSs axis starting from $H_{\text{ext}} = 5 \text{ kOe}$ and decreased up to saturation along the opposite direction with the field step of 10 Oe .

In order to find a ground state at each H_{ext} value, two Mumax3 functions, relax and minimize, were used. To find an energy minimum of the system, the relax function is running. Once the total energy reaches a numerical noise level, the magnitude of the torque is being monitored instead, until it cuts into the numerical noise floor, as well. To increase the probability of finding the lowest energy state, we used then second function, which reaches the minimal energy state by employing the conjugate gradient method to detect even very small changes in energy. The simulated hysteresis loops of the magnetization reversal process of a single wide and narrow NSs are presented in Fig. 8(a) and the values of H_{sw} are listed in the Table I. We can see the reduction of magnetization approximately $0.1-0.2M_S$ at the beginning of the magnetization reversal process. It is attributed to appearance of the closure domains at the edges of NS, as presented in Figs. 8(b) and 8(e), for wide and narrow NS, respectively. The domains expand slowly with decrease of H_{ext} , reaching its maximum state just before the remagnetization [Figs. 8(c) and 8(f)]. Then, the magnetization reversal process happens just at one field step. After remagnetization, we can still record remanent closure domains at the edges [Figs. 8(d) and 8(g)], which shrink with the increase of the H_{ext} .

[1] A. Imre, G. Csaba, L. Ji, A. Orlov, G. H. Bernstein, and W. Porod, *Science* **311**, 205 (2006).

[2] L. J. Heyderman and R. L. Stamps, *J. Phys.: Condens. Matter* **25**, 363201 (2013).

- [3] A. Haldar, D. Kumar, and A. O. Adeyeye, *Nat. Nanotechnol.* **11**, 437 (2016).
- [4] P. Gypens, J. Leliaert, and B. Van Waeyenberge, *Phys. Rev. Appl.* **9**, 034004 (2018).
- [5] J. Dubowik, *Phys. Rev. B* **54**, 1088 (1996).
- [6] N. Rougemaille, F. Montaigne, B. Canals, M. Hehn, H. Riahi, D. Lacour, and J.-C. Toussaint, *New J. Phys.* **15**, 035026 (2013).
- [7] N. Rougemaille, F. Montaigne, B. Canals, A. Duluard, D. Lacour, M. Hehn, R. Belkhou, O. Fruchart, S. El Moussaoui, A. Bendounan, and F. Maccherozzi, *Phys. Rev. Lett.* **106**, 057209 (2011).
- [8] Y. Perrin, B. Canals, and N. Rougemaille, *Nature (London)* **540**, 410 (2016).
- [9] A. Farhan, C. F. Petersen, S. Dhuey, L. Anghinolfi, Q. H. Qin, M. Saccone, S. Veltens, C. Wuth, S. Gliga, P. Mellado, M. J. Alava, A. Scholl, and S. van Dijken, *Nat. Commun.* **8**, 995 (2017).
- [10] E. Ostman, H. Stopfel, I.-A. Chioar, U. B. Arnalds, A. Stein, V. Kapaklis, and B. Hjorvarsson, *Nat. Phys.* **14**, 375 (2018).
- [11] K. J. Kirk, J. N. Chapman, and C. D. W. Wilkinson, *Appl. Phys. Lett.* **71**, 539 (1997).
- [12] G. Yi, P. R. Aitchison, W. D. Doyle, J. N. Chapman, and C. D. W. Wilkinson, *J. Appl. Phys.* **92**, 6087 (2002).
- [13] J. Gadbois and J.-G. Zhu, *IEEE Trans. Magn.* **31**, 3802 (1995).
- [14] J. Deak and R. Koch, *J. Magn. Magn. Mater.* **213**, 25 (2000).
- [15] M. T. Bryan, D. Atkinson, and R. P. Cowburn, *Appl. Phys. Lett.* **85**, 3510 (2004).
- [16] B. Pfau, C. M. Günther, E. Guehrs, T. Hauet, T. Hennen, S. Eisebitt, and O. Hellwig, *Appl. Phys. Lett.* **105**, 132407 (2014).
- [17] K. J. Kirk, J. N. Chapman, S. McVitie, P. R. Aitchison, and C. D. W. Wilkinson, *J. Appl. Phys.* **87**, 5105 (2000).
- [18] S. Vock, C. Hengst, Z. Sasvari, R. Schafer, L. Schultz, and V. Neu, *J. Phys. D* **50**, 475002 (2017).
- [19] S. Zhang, J. Li, J. Bartell, X. Ke, C. Nisoli, P. E. Lammert, V. H. Crespi, and P. Schiffer, *Phys. Rev. Lett.* **107**, 117204 (2011).
- [20] K. J. Kirk, M. R. Scheinfein, J. N. Chapman, S. McVitie, M. F. Gillies, B. R. Ward, and J. G. Tennant, *J. Phys. D* **34**, 160 (2001).
- [21] V. Bhat, B. Farmer, N. Smith, E. Teipel, J. Woods, J. Sklenar, J. Ketterson, J. Hastings, and L. D. Long, *Physica C* **503**, 170 (2014).
- [22] V. Brajuskovic, F. Barrows, C. Phatak, and A. K. Petford-Long, *Sci. Rep.* **6**, 34383 (2016).
- [23] F. Montoncello, L. Giovannini, B. Farmer, and L. D. Long, *J. Magn. Magn. Mater.* **423**, 158 (2017).
- [24] D. Shi, Z. Budrikis, A. Stein, S. A. Morley, P. D. Olmsted, G. Burnell, and C. H. Marrows, *Nat. Phys.* **14**, 309 (2018).
- [25] C. Forestiere, G. Miano, C. Serpico, M. d'Aquino, and L. Dal Negro, *Phys. Rev. B* **79**, 214419 (2009).
- [26] J. Rychly, S. Mieszczyk, and J. Klos, *J. Magn. Magn. Mater.* **450**, 18 (2018).
- [27] V. S. Bhat and D. Grundler, *Phys. Rev. B* **98**, 174408 (2018).
- [28] C. H. Costa and M. S. Vasconcelos, *J. Appl. Phys.* **115**, 17C115 (2014).
- [29] A. P. Valeriano, C. H. Costa, and C. G. Bezerra, *J. Magn. Magn. Mater.* **456**, 228 (2018).
- [30] J. Rychly, J. W. Klos, M. Mruczkiewicz, and M. Krawczyk, *Phys. Rev. B* **92**, 054414 (2015).
- [31] J. Rychly, J. W. Klos, and M. Krawczyk, *J. Phys. D* **49**, 175001 (2016).
- [32] L. G. C. Melo, T. R. B. S. Soares, and O. P. V. Neto, *IEEE Trans. Magn.* **53**, 1 (2017).
- [33] V.-D. Nguyen, Y. Perrin, S. Le Denmat, B. Canals, and N. Rougemaille, *Phys. Rev. B* **96**, 014402 (2017).
- [34] A. Concha, D. Aguayo, and P. Mellado, *Phys. Rev. Lett.* **120**, 157202 (2018).
- [35] Narrow and wide NSs can be treated as S_0 and S_1 initial Fibonacci words (initial “sequences”), respectively. Using iteration rule $S_n = S_{n-1} + S_{n-2}$, where the symbol $+$ means the concatenation of two words (sequence), we can generate subsequent words (sequences).
- [36] R. I. Joseph and E. Schlömann, *J. Appl. Phys.* **36**, 1579 (1965).
- [37] H. Fukushima, Y. Nakatani, and N. Hayashi, *IEEE Trans. Magn.* **34**, 193 (1998).
- [38] A. Vansteenkiste, J. Leliaert, M. Dvornik, M. Helsen, F. Garcia-Sanchez, and B. Van Waeyenberge, *AIP Adv.* **4**, 107133 (2014).
- [39] U. Hartmann, *Phys. Rev. B* **36**, 2331 (1987).
- [40] The abrupt switching of the magnetization in the NSs formed the ribbons found confirmation also in MFM images, were only fully magnetized stripes, apart of small areas at the edges, have been recorded.
- [41] N. Metropolis, A. W. Rosenbluth, M. N. Rosenbluth, A. H. Teller, and E. Teller, *J. Chem. Phys.* **21**, 1087 (1953).
- [42] D. P. Landau and K. Binder, *A guide to Monte Carlo Simulations in Statistical Physics* (Cambridge University Press, New York, 2014).
- [43] Y. Shevchenko, A. Makarov, and K. Nefedev, *Phys. Lett. A* **381**, 428 (2017).
- [44] Y. A. Shevchenko, A. G. Makarov, P. D. Andriushchenko, and K. V. Nefedev, *J. Exp. Theor. Phys.* **124**, 982 (2017).
- [45] F. Wang and D. P. Landau, *Phys. Rev. Lett.* **86**, 2050 (2001).
- [46] V. Y. Kapitan and K. V. Nefedev, in *Modeling, Simulation and Optimization of Complex Processes - HPSC 2012*, edited by H. G. Bock, X. P. Hoang, R. Rannacher, and J. P. Schlöder (Springer International Publishing, Cham, 2014), pp. 95–107.
- [47] K. V. Nefedev and V. Kapitan, in *Advanced Measurement and Test III*, Advanced Materials Research Vol. 718 (Trans Tech, Zurich-Durnten, 2013), pp. 69–73.
- [48] S. Goolaup, A. O. Adeyeye, N. Singh, and G. Gubbiotti, *Phys. Rev. B* **75**, 144430 (2007).
- [49] G. Gubbiotti, S. Tacchi, G. Carlotti, P. Vavassori, N. Singh, S. Goolaup, A. O. Adeyeye, A. Stashkevich, and M. Kostylev, *Phys. Rev. B* **72**, 224413 (2005).
- [50] A. J. Bennett and J. M. Xu, *Appl. Phys. Lett.* **82**, 3304 (2003).
- [51] Ó. Iglesias-Freire, M. Jaafar, L. Pérez, O. de Abril, M. Vázquez, and A. Asenjo, *J. Magn. Magn. Mater.* **355**, 152 (2014).
- [52] A. A. Fraerman and M. V. Sapozhnikov, *Phys. Rev. B* **65**, 184433 (2002).